THE JOURNAL OF BIOLOGICAL CHEMISTRY VOL. 287, NO. 10, pp. 7487–7494, March 2, 2012


# Functional Characterization of a Novel Aquaporin from *Dictyostelium discoideum* Amoebae Implies a Unique Gating Mechanism*

Received for publication, November 30, 2011, and in revised form, January 4, 2012 Published, JBC Papers in Press, January 18, 2012, DOI 10.1074/jbc.M111.329102

**Julia von Bülow[‡], Annika Müller-Lucks[‡], Lei Kai[§], Frank Bernhard[§], and Eric Beitz[‡1]**

*From the [‡]Department of Medicinal and Pharmaceutical Chemistry, Christian-Albrechts-University of Kiel, 24118 Kiel, Germany and the [§]Center for Biomolecular Magnetic Resonance, Institute for Biophysical Chemistry, Goethe-University of Frankfurt/Main, 60438 Frankfurt, Germany*

**Background:** Aquaporins are involved in osmoregulation and cell motility. Functional *D. discoideum* aquaporins are missing.
**Results:** We characterized a putatively gated aquaporin from amoebae that localizes to vacuolar structures, the plasma membrane, and protrusions.
**Conclusion:** Localization and gating hint at functions in osmoregulation and motility.
**Significance:** We identified a novel player in basic physiology of the model organism *D. discoideum*.

**The social amoeba *Dictyostelium discoideum* is a widely used model organism for studying basic functions of protozoan and metazoan cells, such as osmoregulation and cell motility. There is evidence from other species that cellular water channels, aquaporins (AQP), are central to both processes. Yet, data on *D. discoideum* AQPs is almost absent. Despite cloning of two putative *D. discoideum* AQPs, WacA, and AqpA, water permeability has not been shown. Further, WacA and AqpA are expressed at the late multicellular stage and in spores but not in amoebae. We cloned a novel AQP, AqpB, from amoeboidal *D. discoideum* cells. Wild-type AqpB was impermeable to water, glycerol, and urea when expressed in *Xenopus laevis* oocytes. Neither stepwise truncation of the N terminus nor selected point mutations activated the water channel. However, mutational truncation by 12 amino acids of an extraordinary long intracellular loop induced water permeability of AqpB, hinting at a novel gating mechanism. This AqpB mutant was inhibited by mercuric chloride, confirming the presence of a cysteine residue in the selectivity filter as predicted by our structure model. We detected AqpB by Western blot analysis in a glycosylated and a non-glycosylated form throughout all developmental stages. When expressed in *D. discoideum* amoebae, AqpB-GFP fusion constructs localized to vacuolar structures, to the plasma membrane, and to lamellipodia-like membrane protrusions. We conclude that the localization pattern in conjunction with channel gating may be indicative of AqpB functions in osmoregulation as well as cell motility of *D. discoideum.***

AQPs[2] are ubiquitous channel proteins of about 30 kDa that facilitate the selective transmembrane transport of water (orthodox AQPs) (1) or of small uncharged solutes, such as glycerol (2), carbonyls (3), urea (4), and ammonia (5) (aquaglyceroporins). The underlying structure-function relationships in terms of pore selectivity and cation exclusion mechanisms have been largely elucidated by mutational analysis and molecular dynamics simulations on the basis of crystal data (6–8). These studies have identified two filter regions within the conducting channel: the selectivity filter or aromatic/arginine region at the extracellular pore entry that selects passing molecules by size and repels positive ions, and the Asn-Pro-Ala (NPA) region in the pore center which, in conjunction with the aromatic/arginine region, constitutes the cation filter for perfect exclusion of protons and alkali cations. On a cellular level, however, the roles of AQPs are less clear and probably rather diverse in both metazoa and unicells. Various physiological functions are attributed to AQPs, including cell volume sensing/regulation via water permeability (9, 10), compensation of osmotic stress by accumulation or release of compatible solutes (11), and expulsion of toxic metabolites such as ammonia or arsenite (12, 13), to name a few. AQPs have further been reported to be involved in cell motility (14). It is hypothesized that cellular water permeability in concert with an increase of osmolality because of actin depolymerization and ion influx at the leading edge facilitates the formation of lamellipodia, *i.e.* a characteristic feature of migrating cells. An alternative, less investigated process of amoeboidal cell motility involves a different type of larger spherical protrusions, so-called blebs (15). The contribution of AQPs to bleb formation is unknown.

The social amoeba *Dictyostelium discoideum* is a versatile and well established model system for studying basic cellular functions, including osmoregulation and cell migration (16). Yet, physiological and functional data on AQPs in this organism are almost absent. *D. discoideum* uniquely links unicellularity and multicellularity in a complex but controllable life cycle (17).

* This work was supported by the Deutsche Forschungsgemeinschaft (to E. B.).
[1] To whom correspondence should be addressed: Pharmaceutical Institute, University of Kiel, Gutenbergstrasse 76, 24118 Kiel, Germany. Tel.: 49-431-880-1809; Fax: 49-431-880-1352; E-mail: ebeitz@pharmazie.uni-kiel.de.
[2] The abbreviations used are: AQP, aquaporin; AqpA, *D. discoideum* AQP-like protein; PfAQP, *P. falciparum* aquaglyceroporin; PIP2;1, family of plant plasma membrane aquaporins; TIP1;1, family of plant tonoplast aquaporins; WacA, *D. discoideum* AQP-like protein.

It dwells as single amoeboidal cell that detects and actively tracks bacteria by sensing folate. An amoeba can further signal the lack of nutrients by secreting cAMP as a chemotactic agent to surrounding cells, which then migrate toward the cAMP gradient. An aggregate of about 50,000 cells undergoes several stages of different, well defined morphology and eventually forms a stalk carrying a spore.

We set out to analyze AQP expression and functionality in *D. discoideum* amoebae. So far, two putative AQPs, *i.e.* AqpA (18) and WacA (19), have been described only in late multicellular forms and spores of *D. discoideum.* AqpA maintains spore viability during dormancy, whereas the function of WacA is unclear. However, neither protein was shown to conduct water. Here, we describe the identification and functional characterization of a novel AQP, AqpB, which is constitutively expressed in *D. discoideum* amoebae and all other developmental stages. Wild-type AqpB was not functional as a water channel when expressed in *Xenopus laevis* oocytes but was activated by mutational truncation of an intracellular loop, indicating a novel AQP gating mechanism. Localization of an AqpB-GFP fusion protein in *D. discoideum* vacuolar structures, the plasma membrane, and membrane protrusions hints at functions in osmoregulation as well as in cell migration.

## EXPERIMENTAL PROCEDURES

*D. Discoideum Culture and Preparation of cDNA*—Amoeboidal *D. discoideum* AX2 cells were cultured axenically at 22 °C (20). For cDNA preparation, $10^7$ amoebae were harvested in the late-logarithmic phase and lysed in 1 ml of TRIzol (Invitrogen). Total RNA was isolated according to the TRIzol protocol. The RNA was isopropanol-precipitated, washed with ethanol 70%, and dried for cDNA synthesis (First Strand cDNA synthesis kit, Fermentas) using $(dT)_{18}$ primers.

*Cloning of aqpB, Mutagenesis, and cRNA Preparation*—The coding sequence of *aqpB* was amplified by PCR from *D. discoideum* amoebae cDNA. The PCR product was blunted and ligated into EcoR V-digested pBluescript II SK(–) for sequencing. DNA point mutations were introduced according to the QuikChange protocol (Stratagene), and truncations were generated by PCR with respective primers. For the generation of GFP-fusion constructs, *aqpB* was ligated into pDXA-GFP2 (Dictybase Stock Center) using either the BamH I/XhoI sites (N-terminal GFP) or, after removal of the *aqpB* stop codon, using the HinD III/KpnI sites (C-terminal GFP). For cell-free production of AqpB, the coding sequence was ligated into pET21a via BamH I/XhoI, generating a construct encoding a C-terminal $His_{10}$ purification tag. Details on the used PCR and mutation primers are available from the authors. For cRNA synthesis, *aqpB* wild-type and mutant DNA was ligated into pOG2 (21) via the XbaI/HinD III restriction sites resulting in constructs coding for a N-terminal HA epitope tag. cRNA transcription was done using the NotI linearized plasmid and T7-RNA-polymerase (mMESSAGE mMACHINE, Ambion).

*Expression of aqpB and Permeability Assays Using Xenopus laevis oocytes*—Oocyte preparation, injection, and permeability assays were done as described earlier (21). Briefly, stage V and VI *X. laevis* oocytes were defolliculated by collagenase A treatment (Roche) and injected with 50 nl of ND96 buffer (96 mM NaCl, 2 mM KCl, 1.8 mM $CaCl_2$, 1 mM $MgCl_2$, 5 mM HEPES (pH 7.4)) or with 50 nl of cRNA (100 ng/$\mu$l). The oocytes were incubated for 3 days at 16 °C. Water permeability was measured by transferring the oocytes into 1:3 diluted ND96 buffer. For isoosmotic solute permeability measurements, 65 mM NaCl were isotonically substituted by 130 mM glycerol or urea. The assays were carried out at room temperature with video monitoring and calculation of the relative volume increase on the basis of the oocyte-covered area. The susceptibility for mercury inhibition was tested by addition of 300 $\mu$M $HgCl_2$ to the incubation buffer 15 min prior to the assay. The osmotic water permeability ($P_f$ in $\mu$m/s) was calculated from the oocyte surface area (S = 0.045 $cm^2$), the initial oocyte volume ($V_0 = 9 \times 10^{-4}$ $cm^3$), the initial slope of the volume increase ($d(V/V_0)/dt$, in s), the molecular water volume ($V_w$ = 18 $cm^3$ /mol), and the osmotic gradient ($osm_{in}$ - $osm_{out}$) by the following equation: $P_f = V_0 \times d(V/V_0)/dt/[S \times V_w \times (osm_{in} - osm_{out})]$. Solute permeability coefficients ($P_{sol}$) were calculated from the following equation: $P_{sol} = sol_{tot} \times V_0 \times d(V/V_0)/dt/[S \times (sol_{out} - sol_{in})]$, considering the total solute concentration of the system ($sol_{tot}$ = 300 mM) and the solute gradient ($sol_{out}$ - $sol_{in}$) of 130 mM.

*Cell-free Production of AqpB, Proteoliposome Reconstitution, and Stopped-flow Light Scattering*—AqpB was produced according to prior protocols (22, 23) using 2-ml reactors (24). The reaction mix was supplied with 0.1% of Brij-35 for membrane protein solubilization during incubation at 30 °C for approx. 20 h with gentle shaking. AqpB was affinity-purified in one step by immobilized metal-chelated affinity chromatography. Solubilized AqpB was bound overnight to $Ni^+$-loaded resin slurry (Qiagen) at 4 °C with gentle shaking, loaded onto a column, washed with 10 volumes of column buffer (20 mM Tris-HCl (pH 7.8), 300 mM NaCl, 0.05% *n*-Dodecyl-$\beta$-D-maltoside (DDM)) supplemented with 80 mM imidazole and eluted with column buffer supplemented with 300 mM imidazole. For reconstitution into liposomes, chloroform-solubilized *Escherichia coli* polar lipids (Avanti Polar Lipids) were transferred to a round-bottom flask. A thin lipid film was formed by chloroform evaporation under a nitrogen stream. 1 ml of 100 mM MOPS (pH 7.5) was added to form a 20 mg/ml multilamellar vesicle suspension by vortexing for 15 min. The suspension was passed at least 21 times through a 200-nm Whatman polycarbonate membrane filter. The resulting unilamellar liposome suspension was used for AqpB reconstitution as described previously (25). Briefly, a reconstitution mixture was prepared at room temperature by sequentially adding reconstitution buffer (100 mM MOPS, 4 mM Triton X-100 (pH 7.5)), 20 mg/ml preformed liposomes (final concentration 4 mg/ml), and 100 $\mu$g/ml purified AqpB. The mixture was incubated at room temperature with gentle shaking for 30 min. The detergent was removed using SM-2 beads (Bio-Rad), and the proteoliposomes were collected twice at 500,000 $\times$ *g* for 45 min with an intermediate washing step with reconstitution buffer. Finally, the proteoliposomes were resuspended in 1.6 ml of reconstitution buffer. Water permeability was assayed in a hypertonic gradient of 200 mosm/kg (reconstitution buffer with added sucrose) using a stopped-flow apparatus (26).

*D. discoideum Amoebae Membrane Protein Preparation, Glycosylation Analysis, and Developmental Cycle Sampling*—*D. discoideum* amoebae were harvested (2000 × *g*, 4 °C, 10 min), washed twice with Sörensen phosphate buffer (15 mM $KH_2PO_4$, 2 mM $Na_2HPO_4$ (pH 6.0)) and lysed by four freeze-thaw cycles at −80 °C (8 min) and 37 °C (6 min). The total protein was quantified using the Bradford assay (Bio-Rad). Cell debris was removed (10,000 × *g*, 4 °C, 15 min), and the membrane protein fraction was collected (100,000 × *g*, 4 °C, 45 min). *N*-glycosylation of AqpB was assayed by incubation with 1000 units of *N*-glycosidase F (New England Biolabs) for 60 min at 37 °C. Chemical deglycosylation was done by incubating 1 mg of lyophilized *D. discoideum* membrane protein with 140 μl ice-cold trifluoromethanesulfonic acid (> 99%) and 15 μl of anisole for 3 h on ice. For neutralization, pyridine was added to 60% and the protein was precipitated by addition of 5% trichloroacetic acid (27). To initiate the developmental cycle, *D. discoideum* amoebae of the late-logarithmic phase were harvested (1000 × *g*, 4 °C, 5 min), washed twice with 20 ml Sörensen phosphate buffer and resuspended to $10^8$ cells/ml. 400 μl of the cell suspension was put on each nitrocellulose filter and incubated at 22 °C in a moist chamber. Cells were harvested at 4-h intervals for 24 h using 10 ml of phosphate buffer (14 mM $KH_2PO_4$, 4.8 mM $K_2HPO_4$ (pH 6.7)), collected (1000 × *g*, 4 °C, 5 min), and disrupted by 15 passages through a syringe with a 23-gauge needle.

*Western Blot Analyses*—For protein detection we used a commercial monoclonal anti-hemagglutinin antibody (Santa Cruz Biotechnology) and an affinity-purified polyclonal antiserum directed against the N-terminal peptide at positions 20–34 of AqpB (BioGenes, Berlin, Germany) (Fig. 1*A*). Membrane proteins from *Xenopus* oocytes equivalent to one or 1/10 oocyte per lane or from *D. discoideum* cells (10 μg per lane) were separated by SDS-PAGE and transferred to PVDF membranes (Macherey & Nagel). The membranes were incubated with primary antibody (1:5000) and detected with horseradish peroxidase-conjugated goat anti-mouse or goat anti-rabbit antisera (Jackson ImmunoResearch Laboratories) using ECL Plus (Amersham Biosciences). The specificity of the anti-AqpB antiserum was tested by a 1-h preincubation with 1 μg/ml of the immunizing peptide corresponding to a 10-fold excess.

*Expression and Localization of AqpB-GFP Fusion Constructs*—$4 \times 10^7$ *D. discoideum* amoebae were harvested (1000 × *g*, 4 °C, 5 min), washed twice with electroporation buffer (10 mM $KH_2PO_4$, 50 mM sucrose (pH 6.1)) and incubated for 5 min in 300 μl of electroporation buffer with 6 μg of plasmid DNA. Electroporation was done in a 0.4-mm electroporation cuvette with two pulses (5-s delay) of 1 kV, 25 μF, and a time constant of 0.6–1 ms using a Gene Pulser II (Bio-Rad). After 10 min at room temperature, 3 μl of a $CaCl_2/MgCl_2$ solution (0.1 M each) was added, and cells were incubated for another 15 min while shaking at 150 min. After addition of 10 ml of axenic medium, cells were incubated at 22 °C for 24 h. Fluorescence imaging was done by confocal laser scanning microscopy (LSM 510, Zeiss) with living amoebae in Sörensen phosphate buffer at an excitation wavelength of 475 nm.

## RESULTS

*Cloning and Sequence Analysis of D. discoideum AqpB*—BLAST searches in the genome sequence of *D. discoideum* yielded a novel putative AQP (DDB_G0279443). The intronless ORF is located on chromosome 3 and consists of 885 bp with an A + T content of 62%. The flanking non-coding regions have an A + T content of more than 80%, which is typical for intergenic regions in the *D. discoideum* genome (28). We were able to amplify the ORF from cDNA of *D. discoideum* AX2 amoebae, indicating that DDB_G0279443 is transcribed and does not represent a pseudogene. The obtained sequence was identical to the database entry. Expressed sequence tag data from cells of the multicellular slug form provide further support for gene transcription. Hence, in succession to the previously described *aqpA* (18) and according to the dictybase nomenclature convention, we refer to DDB_G0279443 now as *aqpB* and to the encoded protein as AqpB.

Sequence comparisons indicate a higher similarity of AqpB with water-specific AQPs, *e.g.* from plants (TIP1;1 from *Arabidopsis thaliana*, Ref. 29) or mammals (AQP1, Ref. 1) with 30% identical and 48% similar residues. A topology prediction of AqpB on the basis of the crystal structure of mammalian AQP1 (PDB code 1J4N, Ref. 30) reveals the typical set of six transmembrane helices (Fig. 1*A*), two canonical NPA motifs at positions 106–108 and 251–253 (labeled *green* in Fig. 1*A*), and an aromatic/arginine region around Arg-254 (labeled *yellow*). A structure model of the selectivity filter as viewed top-down is shown in Fig. 1*B*. Besides the arginine, its composition shows neither the typical residues of water-specific AQPs nor those of aquaglyceroporins, prohibiting reasonable estimations on pore selectivity and, thus, prompted experimental analysis. We also identified multiple consensus sites for secondary protein modifications of AqpB. In particular, the putative PKA phosphorylation site at Ser-120 of loop B is reminiscent of plant AQPs of the plasma membrane intrinsic protein family 2;1 (PIP2;1), in which phosphorylation of an analogous serine is reported to regulate channel gating (31). We further located consensus sites for *O*-glycosylation at Ser-75 (predicted by the Dicty-O-Glyc algorithm, Ref. 32) and *N*-glycosylation at Asn-262 (N-*X*-S/T motif). Other structural features that required experimental evaluation were the ambiguity concerning two potential start methionines (Met-1 and Met-18), the extraordinary long intracellular loop D (35 amino acids compared with 11 amino acids in AQP1, Ref. 30), and the presence of a negatively charged Asp-275 within transmembrane domain 6, *i.e.* a position that holds a proline in each of the remaining known AQPs.

*Wild-type AqpB Is Not Functional in Xenopus laevis Oocytes*—For functional analysis, we expressed N-terminally HA-tagged AqpB in *Xenopus* oocytes. A respective AqpB protein band of 36 kDa was detected in the oocyte membrane fraction (Fig. 2*A*). A second band of 29 kDa was detected, fitting in size a translation start at Met-18 (Fig. 1*A*). Buffer-injected oocytes and oocytes expressing the highly conducting water-specific rat AQP1 and the aquaglyceroporin from *Plasmodium falciparum*, PfAQP, served as controls in the permeability assays. The oocytes were abruptly subjected to

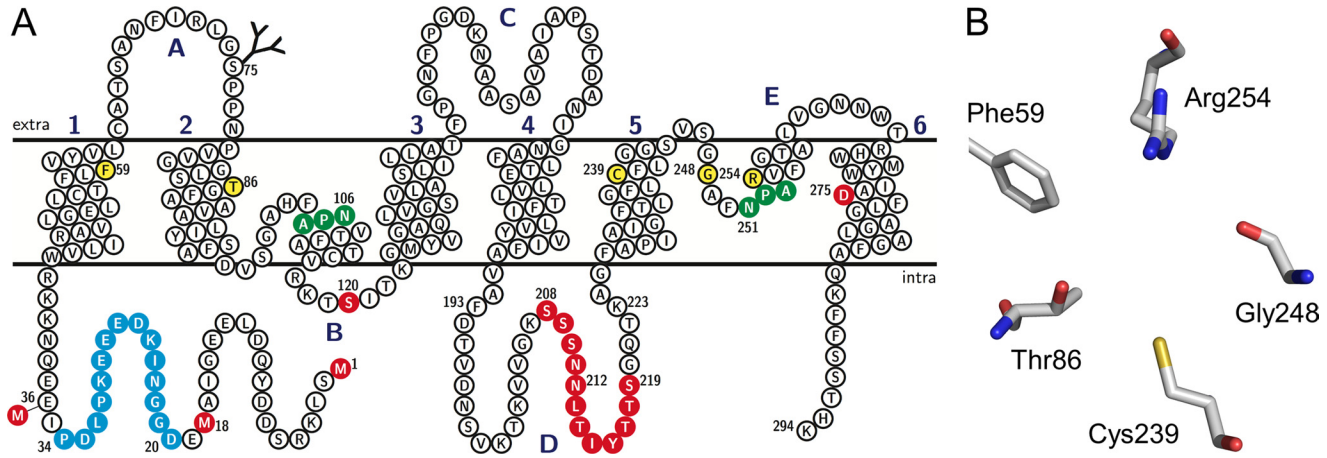


FIGURE 1. **Topology and structure predictions of AqpB.** *A*, the topology plot of AqpB is on the basis of the crystal structure of mammalian AQP1 (PDB code 1J4N) and highlights the Asn-Pro-Ala (NPA) signature motifs in *green*, the putative residues of the selectivity filter in *yellow*, and a predicted *O*-glycosylation site (Ser-75). The peptide sequence used for generation of an antiserum is shown in *blue*. Sites modified in this study by point mutation and for truncations of the N terminus and loop D are labeled in *red*. The plot was generated using TeXtopo (46). *B*, a structure prediction of the selectivity filter of AqpB is shown as viewed from the extracellular side down the channel. The model was generated using PyMOL.

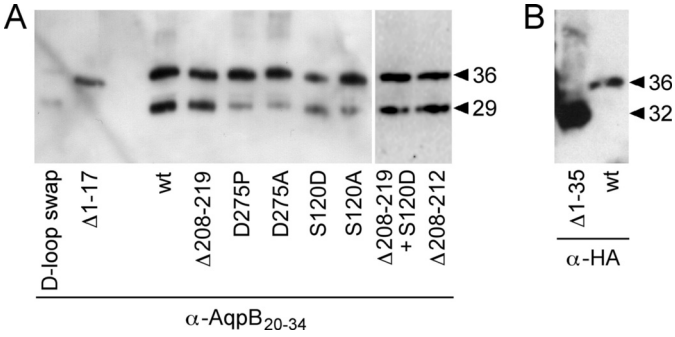


FIGURE 2. **Expression of HA-tagged AqpB wild-type and mutants in *X. laevis* oocytes.** Western blot analysis was done using the membrane protein fraction from one or 1/10 oocyte (*A*, *two right lanes*). An antiserum directed against the N-terminal peptide (positions 20–34) of AqpB was used (*A*) or, for the Δ1–35 mutant lacking this peptide, an anti-HA antibody (*B*). The anti-HA antibody detects only full-length proteins. Hence, single bands are seen. The apparent molecular mass in kDa is indicated.

inward-directed osmotic (140 mosm/kg) or isotonic solute gradients (130 mM glycerol or urea). In these assays, AqpB showed neither water (Fig. 3*A*) nor glycerol or urea permeability (*B*) above buffer-injected oocytes, whereas AQP1 and PfAQP exhibited typical high permeability rates (21).

To test whether the HA-tag added to AqpB was responsible for the lack of function, we expressed an untagged AqpB. Detection with an AqpB-specific antibody that showed two bands of 31 kDa and 29 kDa (Fig. 4*A*), indicating that in oocytes both potential AqpB start sites at Met-1 and Met-18 (Fig. 1*A*) are used. We additionally generated and expressed two N-terminally truncated forms of AqpB: Δ1–17 to ensure expression of only the short form of AqpB and Δ1–35, carrying an artificial start methionine to shorten the length of the N terminus to that of mammalian AQP1 (Fig. 1*A*). Despite good expression in oocytes, neither untagged variant of AqpB showed water permeability (Fig. 2, *A* and *B*). Another attempt to activate wild-type AqpB was to shift the acidity of the assay buffer to pH 5.2 because some AQPs are regulated by pH, *e.g. h*AQP6 (by external acidity, Ref. 33) or SoPIP2;1 (internal acidity, Ref. 31). Yet, AqpB remained impermeable to water.

*Truncation of the Intracellular Loop D Turns AqpB into an Active Water Channel*—Because neither the N terminus of AqpB nor the protonation status seemed to affect channel permeability, we first addressed the putative PKA phosphorylation site at Ser-120 and the atypical Asp-275 in transmembrane domain 6 by generating point mutations. We changed Ser-120 to asparagine (S120D) and alanine (S120A) to mimic a permanently phosphorylated or unphosphorylated state, respectively, and replaced Asp-275 by proline (D275P) and alanine (D275A). Both Ser-120 mutants and even the AqpB variants carrying the structurally challenging exchanges of Asp-275 in the hydrophobic environment of transmembrane domain 6 were well expressed in oocytes (Fig. 2). However, the mutations did not induce water permeability in AqpB.

We then focused on the extraordinarily long loop D of AqpB (Fig. 1*A*). We chose the sequence stretch from positions 208 to 219 for deletion because these 12 amino acids alone contain eight residues with hydroxyl moieties and, thus, have a high potential for regulation by phosphorylation. AqpB Δ208–219 was expressed in oocytes at levels comparable with wild-type AqpB (Fig. 2). Subsequent osmotic swelling assays with AqpB Δ208–219 yielded six times higher water permeability rates than with non-expressing oocytes (Fig. 3*A*), translating into an intermediate water permeability coefficient, $P_f$, of 51 $\mu$m/s. Glycerol and urea did not pass AqpB Δ208–219 (Fig. 3*B*). This shows that the channel interior of AqpB is compatible with water-specific conduction and further hints at a closing function of the intracellular loop D.

We confirmed water permeability of AqpB Δ208–219 by production of the C-terminally $His_{10}$-tagged protein in an *E. coli*-based cell-free system, reconstitution of the purified protein in liposomes, and testing for water permeability by stopped-flow light scattering. This approach also ensured that the obtained protein was devoid of secondary modifications. The shrinkage rates in hypertonic buffer of proteoliposomes carrying AqpB Δ208–219 ($\tau$ = 15 ms) were five times higher than those of empty liposomes ($\tau$ = 70 ms), perfectly reflecting the data obtained with the oocytes (Fig. 3*C*).

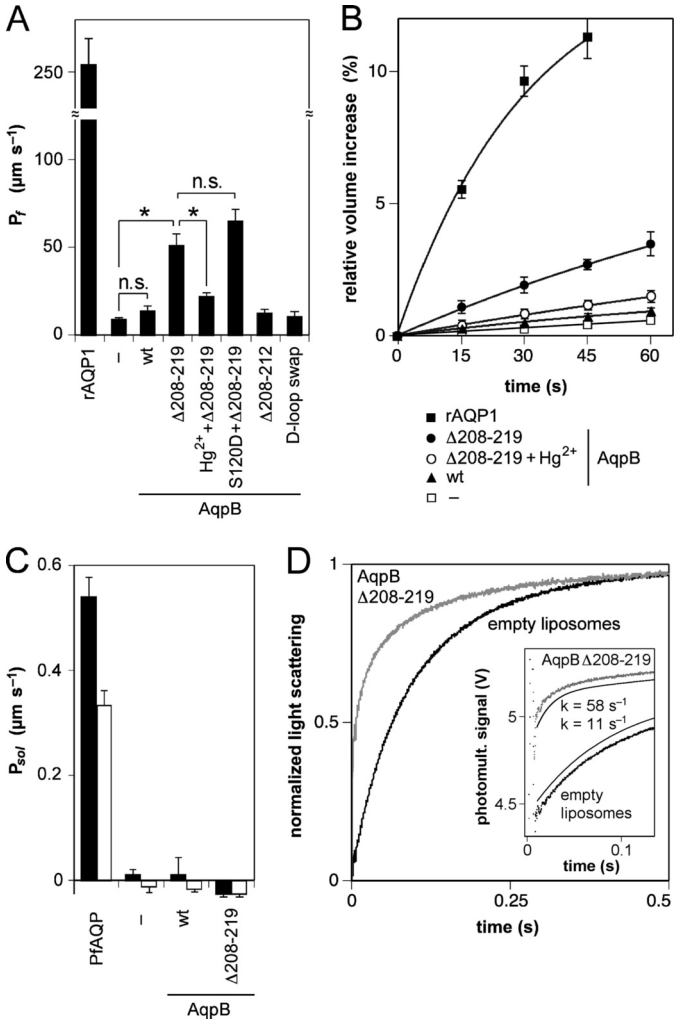


FIGURE 3. **Functional analysis of AqpB wild-type and mutants.** *A*, the water permeability of AqpB wild-type and mutants in comparison to rat AQP1 (*rAQP1*) expressing *X. laevis* ooctyes and to buffer-injected oocytes (–). The AqpB Δ208–219 mutant was further inhibited by 300 $\mu$m $Hg^{2+}$. The *bars* indicate the permeability coefficient ($P_f$) derived from swelling rates in a 140 mosm/kg inward-directed osmotic gradient. The *error bars* denote the S.E. from 7–10 experiments. *, significantly different $P_f$ values, $p < 0.01$. *n.s.*, non-significant difference. *B*, the original oocyte swelling curves used for the calculation of the $P_f$ values are shown. The data points (± S.E.) are connected by single exponentially fitted curves. *C*, glycerol (*filled bars*) and urea (*open bars*) permeability coefficients ($P_{sol}$ ± S.E.) are plotted as obtained from *X. laevis* oocyte swelling in a 130 mM isotonic chemical gradient. The aquaglyceroporin from *P. falciparum* (*PfAQP*) and buffer-injected oocytes (–) served as controls ($n = 7–10$). *D*, water permeability of AqpB Δ208–219 was confirmed by stopped-flow light scattering with proteoliposomes and empty liposomes in an outward osmotic gradient of 200 mosm/kg. Nine traces were averaged and normalized for each experiment. Reconstitution and assays were repeated twice with equal results. The *inset* depicts the original, non-normalized photomultiplier readings for the first 110 ms. Signal artifacts are seen within the 10-ms dead time. The curves derived from single exponential fits (*smooth lines*) and respective rate constants (*k*) are plotted next to the raw data.

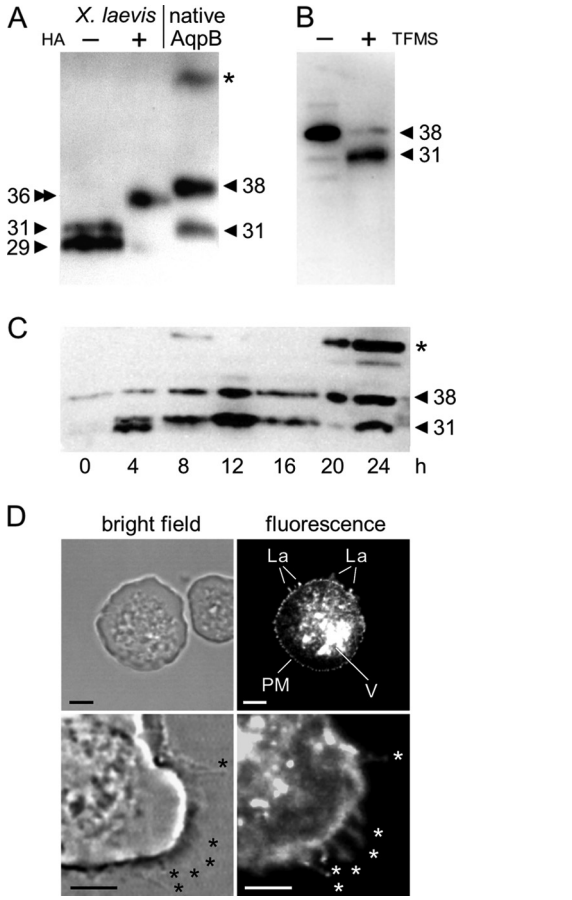


FIGURE 4. **Expression, glycosylation, and localization of AqpB in *D. discoideum*.** *A*, the Western blot analysis using an anti-AqpB antiserum shows native AqpB in comparison to AqpB heterologously expressed in *X. laevis* oocytes with and without an N-terminal HA tag. The apparent molecular masses are indicated (kDa). A 90-kDa band labeled with an *asterisk* is not specific. B, trifluoromethanesulfonic acid (*TFMS*) was used for chemical deglycosylation of native AqpB. The shift in molecular weight from 38 kDa to 31 kDa is shown by Western blot analysis. *C*, the Western blot shows AqpB expression levels during a full developmental cycle of *D. discoideum* over 24 h. Both glycosylated (38 kDa) as well as non-glycosylated AqpB (31 kDa) is seen. An additional smaller band in the 4 h lane corresponds to translation from Met-18 of AqpB. A nonspecific 90-kDa band is labeled with an *asterisk*. *D*, AqpB was localized in *D. discoideum* amoebae by expression of a C-terminal GFP-fusion construct. The *upper panel* (*scale bar* = 5 $\mu$m) shows a bright field image of one transformed (*left panel*) and one untransformed amoeba (*right panel*). In the GFP excitation channel, only the transformed amoeba exhibit fluorescence. Lamellipodia-like protrusions (*La*) of the plasma membrane (*PM*) and intracellular vacuolar structures (*V*) are labeled in the *upper panel*. The *lower panel* shows a higher magnification view for visualization of the plasma membrane protrusions (*asterisks*).

This gain of function opened up the possibility to further investigate the putative gating mechanism of loop D and to test our predicted AqpB structure model. We generated three more loop D mutants (Fig. 1*A*), *i.e.* a full swap of loop D with that of AqpA (replacement of position 193 to 233 by Phe-Asn-Val-Trp-Asp-Arg-Arg), deletion of only five residues (Δ208–212), and combination of Δ208–219 with S120D (Figs. 2 and 3*A*). Swapping of the complete loop D resulted in low expression and a non-functional channel similar to previous experiences with such crude operations (34). Curiously, the short Δ208–212 truncation of AqpB, despite normal expression levels, did not conduct water. This points to the following seven positions from 213 to 219 as the channel-blocking site. However, it cannot be excluded that deletion without replacement of residues changes the overall fold of loop D, which would interfere with a direct identification of the blocking residues. These issues are complex and are currently addressed in ongoing studies. The combination of the phosphorylation mimicry at Ser-120 (S120D) with Δ208–219 was functional and produced similar water permeability as Δ208–219 alone (Fig. 3*A*), showing that Ser-120 is probably not required for channel opening. Our

AqpB structure model predicts a cysteine residue (Cys-239) in the aromatic/arginine selectivity filter region that would most likely render the pore sensitive to mercury inhibition. Incubation of AqpB Δ208–219 expressing oocytes with 300 μM mercuric chloride indeed inhibited water permeability by half (Fig. 3*A*).

*Expression, Glycosylation, and Intracellular Localization of AqpB in Vivo*—Having established a water selective channel layout in AqpB, we tested for *in vivo* expression by Western blot analysis using an affinity-purified anti-AqpB antibody (Fig. 4*A*). We detected two specific bands of 31 and 38 kDa in the total membrane protein fraction of *D. discoideum* amoebae, *i.e.* the first detection of an AQP protein in the single cell state. In some blots, a third 90-kDa band was visible, representing an unspecific signal that remained when the antiserum was blocked with the immunizing peptide. The molecular weight of 31 kDa corresponds to the upper of two bands obtained from *Xenopus* oocytes that heterologously express untagged AqpB (Fig. 4*A*). In a few cases, a smaller 29-kDa band was obtained as well (Fig. 4*C*, *lane at 4 h*), indicating that AqpB translation regulation of *D. discoideum* is somewhat ambiguous, using mainly Met-1 but occasionally Met-18 (Fig. 1*A*). We further figured that the higher 38-kDa band derived from secondary modification of AqpB, presumably by glycosylation. For analysis, we used an enzymatic approach for specific N-deglycosylation and an unspecific chemical deglycosylation protocol. Incubation with *N*-glycosidase F did not shift the molecular weight of AqpB, indicating the absence of *N*-glycosylation. Chemical treatment with trifluoromethanesulfonic acid, however, resulted in a clear band shift from 38 kDa to 31 kDa (Fig. 4*B*), strongly hinting at *O*-glycosylation, probably at the predicted Ser-75 site. A special type of glycosylation of *Dictyostelium* is *O*-phosphoglycosylation (35), which is currently not well predictable. It will be interesting, though, to investigate this further because of the numerous residues with hydroxyl moieties in AqpB.

We then analyzed AqpB expression by Western blot analysis at 4-h intervals, covering a full developmental cycle of *D. discoideum* from amoebae (0–8 h) via the various multicellular stages (8–16 h) to the formation of spores (16–24 h). We detected AqpB protein over the entire sampling period, indicating constitutive stage-independent gene expression (Fig. 4*C*).

When used on fixed *D. discoideum* cells for immunofluorescence detection, our generated anti-AqpB antiserum produced unspecific staining, probably because of binding of the antibody to the 90-kDa protein detected in the Western blot analyses. This rendered our antiserum unsuitable for immunolocalization studies. As an alternative, we used N- and C-terminal AqpB-GFP fusion constructs for localization in *D. discoideum* amoebae. The cells were electroporated with 6 μg of DNA, and images where taken after 24 h by confocal laser scanning microscopy. Fig. 4*D* depicts the intracellular localization of the C-terminal AqpB-GFP fusion protein in a living *D. discoideum* amoeba. Fluorescence was detected in intracellular vacuolar structures, in a punctuate structure within the plasma membrane, and in lamellipodia-like plasma membrane protrusions. Untransformed cells did not fluoresce (Fig. 4*D*, *right cell*). The N-terminal construct showed the same localization pattern, which is consistent with cellular functions of AqpB in osmoregulation and cell motility.

## DISCUSSION

AQPs constitute an ancient family of proteins that are highly conserved throughout all branches of life. We have shown before that the genomes of unicellular organisms encode up to three (*Trypanosoma brucei*) (36), four (*Trypanosoma cruzi*), or even five AQP isoforms (*Leishmania major*) (37). Protozoa expressing only a single AQP (*Plasmodium* spp.) (21) or fully lacking AQP encoding genes (*Cryptosporidium parvum*) (37) appear to be rare exceptions to the rule. Therefore, we expected to find AQP expression in *D. discoideum* amoebae. AqpB represents the first AQP identified in motile *D. discoideum* cells. It came quite as a surprise, however, that AqpB needs activation to conduct water because most AQPs appear to be non-gated channels. On the basis of this finding, it seems adequate to revisit the previously reported putative *D. discoideum* AQPs AqpA and WacA, for which functionality has not yet been shown (18, 19). With regard to our experimental implications of AqpB gating, it may be more than coincidence that the most evident examples of AQP channel gating have been found in fungi and plants and that *Dictyostelia* are phylogenetically situated right between these two genera (38).

The gating mechanisms of fungal AQPs, such as *Saccharomyces cerevisiae* Fps1 and *Pichia pastoris* Aqy1, involve extended N-terminal sequence stretches, as shown by mutational studies. Fps1 is a glycerol-conducting channel that closes under hypertonic conditions by a not fully elucidated molecular mechanism. By closing Fps1, the yeast cell can accumulate freshly synthesized glycerol as a compatible solute for adaptation of the cytosolic osmolality. When the environmental osmolality drops, Fps1 will open, and glycerol is released (39). The physiological function of the water-specific Aqy1 is less clear, but crystallography has revealed a gating mechanism. The N-terminal Tyr-31 flips into the water pore for closure, probably after protein phosphorylation or mechanical stress on the membrane (40). Gating of plant AQPs of the PIP2;1 family depends on pH-dependent protonation and binding of divalent cations (31). Further, effects by phosphorylation of a loop B serine are reported (31). A network of binding sites for protons and cations, such as calcium, have been localized to aspartate and glutamate residues of the N terminus and to a histidine in loop D, with the latter being the major pH sensor site. It is thought that protonation of the histidine alters folding of loop D in a way that it interacts with the N terminus as a joint blocking structure of the channel.

*D. discoideum* AqpB shares structural features with both fungal and plant AQPs. However, stepwise truncation of the AqpB N terminus, pH-shifts, and mimicking of loop B phosphorylation did not activate the pore, whereas truncation of loop D alone led to water permeability. This is indicative of a novel molecular mechanism for AqpB gating with a focus on loop D and, in particular, on the sequence stretch from position 213 to 219.

Osmoregulation in *D. discoideum* amoebae (41) and various other protozoa, such as *Amoeba proteus* (42) and *T. cruzi* (43), involves similar networks of contractile vacuoles and/or acido-

calcisomes. These plant-like organelles actively accumulate high concentrations of protons, pyrophosphate, and calcium via two vacuolar proton pumps, *i.e.* an ATPase and a pyrophosphatase, plus a calcium ATPase. The resulting osmotic gradient draws water into the vacuoles, which periodically fuse with the plasma membrane for water expulsion by contraction. AQPs have been localized to the contractile vacuoles of *T. cruzi* and *A. proteus*, explaining the high water permeability of the vacuolar membranes (42, 43). The intracellular fluorescence pattern of AqpB obtained with *D. discoideum* amoebae may hint at a similar function. There may be differences in terms of regulation on the molecular level because the *T. cruzi* and *A. proteus* AQPs reportedly are non-gated and constitutively open water channels.

The involvement of AQPs in cell motility has been investigated only with mammalian cells. In particular, human AQP1 and AQP5 appear to enhance formation of lamellipodia and boost the spreading of tumor cells (14, 44). The localization of AqpB in lamellipodia-like plasma membrane protrusions of *D. discoideum* amoebae provides first evidence for a role of water permeability in amoeboid motility. An attractive model for AqpB-facilitated induction of lamellipodia would be on the basis of mechanical activation similar to the hypothesized gating of Aqy1 (40). Once a critical degree of membrane curvature has been generated by membrane-deforming proteins, *e.g.* of the Bin/Amphiphysin/Rvs (BAR) family (45), AqpB would open and, in concert with ion fluxes, facilitate osmotic water influx into the structure to further drive formation of the lamellipodium. At plasma membrane sites with normal curvature, AqpB would remain closed and, thus, maintain the osmotic status of the *D. discoideum* cell.

Together, the identification and localization of a functional AQP in *D. discoideum* amoebae fills a gap in *Dictyostelium* research and, because of the wide use of *D. discoideum* as a model system, contributes to the understanding of basic cell physiology. It further provides new insight into molecular AQP regulation mechanisms. The possibility to exploit AqpB channel gating may prove to be a particularly valuable tool, *e.g.* by expressing permanently open or closed AqpB channel mutants, to elucidate the role of water permeability in fundamental cellular processes such as osmoregulation and cell motility.

*Acknowledgments—We thank M. Leippe and R. Dhakshinamoorthy for providing Dictyostelium AX2 cells and for help with the cell culture, and M. Schwake and M. Bleich for support with the Xenopus oocytes. We also thank R. Kaldenhoff for putting his stopped-flow assays stand at our disposal and M. Nelson for assistance with the Dictyostelium development protocol. We also thank the Stock Center at dictybase for providing the pDXA-GFP2 plasmid.*

## REFERENCES

1. Preston, G. M., Smith, B. L., Zeidel, M. L., Moulds, J. J., and Agre, P. (1994) Mutations in aquaporin-1 in phenotypically normal humans without functional CHIP water channels. *Science* **265,** 1585–1587
2. Fu, D., Libson, A., Miercke, L. J., Weitzman, C., Nollert, P., Krucinski, J., and Stroud, R. M. (2000) Structure of a glycerol-conducting channel and the basis for its selectivity. *Science* **290,** 481–486
3. Pavlovic-Djuranovic, S., Kun, J. F., Schultz, J. E., and Beitz, E. (2006) Dihydroxyacetone and methylglyoxal as permeants of the *Plasmodium* aquaglyceroporin inhibit parasite proliferation. *Biochim. Biophys. Acta* **1758,** 1012–1017
4. Echevarria, M., Windhager, E. E., Tate, S. S., and Frindt, G. (1994) Cloning and expression of AQP3, a water channel from the medullary collecting duct of rat kidney. *Proc. Natl. Acad. Sci. U.S.A.* **91,** 10997–11001
5. Holm, L. M., Jahn, T. P., Møller, A. L., Schjoerring, J. K., Ferri, D., Klaerke, D. A., and Zeuthen, T. (2005) NH3 and NH4+ permeability in aquaporin-expressing *Xenopus* oocytes. *Pflueger's Arch.* **450,** 415–428
6. Beitz, E., Wu, B., Holm, L. M., Schultz, J. E., and Zeuthen, T. (2006) Point mutations in the aromatic/arginine region in aquaporin 1 allow passage of urea, glycerol, ammonia, and protons. *Proc. Natl. Acad. Sci. U.S.A.* **103,** 269–274
7. Wu, B., Steinbronn, C., Alsterfjord, M., Zeuthen, T., and Beitz, E. (2009) Concerted action of two cation filters in the aquaporin water channel. *EMBO J.* **28,** 2188–2194
8. de Groot, B. L., and Grubmüller, H. (2001) Water permeation across biological membranes. Mechanism and dynamics of aquaporin-1 and GlpF. *Science* **294,** 2353–2357
9. Thrane, A. S., Rappold, P. M., Fujita, T., Torres, A., Bekar, L. K., Takano, T., Peng, W., Wang, F., Thrane, V. R., Enger, R., Haj-Yasein, N. N., Skare, Ø., Holen, T., Klungland, A., Ottersen, O. P., Nedergaard, M., and Nagelhus, E. A. (2011) Critical role of aquaporin-4 (AQP4) in astrocytic Ca2+ signaling events elicited by cerebral edema. *Proc. Natl. Acad. Sci. U.S.A.* **108,** 846–851
10. Huang, C. G., Lamitina, T., Agre, P., and Strange, K. (2007) Functional analysis of the aquaporin gene family in *Caenorhabditis elegans*. *Am. J. Physiol. Cell Physiol.* **292,** C1867–1873
11. Luyten, K., Albertyn, J., Skibbe, W. F., Prior, B. A., Ramos, J., Thevelein, J. M., and Hohmann, S. (1995) Fps1, a yeast member of the MIP family of channel proteins, is a facilitator for glycerol uptake and efflux and is inactive under osmotic stress. *EMBO J.* **14,** 1360–1371
12. Zeuthen, T., Wu, B., Pavlovic-Djuranovic, S., Holm, L. M., Uzcategui, N. L., Duszenko, M., Kun, J. F., Schultz, J. E., and Beitz, E. (2006) Ammonia permeability of the aquaglyceroporins from *Plasmodium falciparum*, *Toxoplasma gondii* and *Trypansoma brucei*. *Mol. Microbiol.* **61,** 1598–1608
13. Wu, B., Song, J., and Beitz, E. (2010) Novel channel enzyme fusion proteins confer arsenate resistance. *J. Biol. Chem.* **285,** 40081–40087
14. Saadoun, S., Papadopoulos, M. C., Hara-Chikuma, M., and Verkman, A. S. (2005) Impairment of angiogenesis and cell migration by targeted aquaporin-1 gene disruption. *Nature* **434,** 786–792
15. Langridge, P. D., and Kay, R. R. (2006) Blebbing of *Dictyostelium* cells in response to chemoattractant. *Exp. Cell Res.* **312,** 2009–2017
16. Annesley, S. J., and Fisher, P. R. (2009) *Dictyostelium discoideum*. A model for many reasons. *Mol. Cell Biochem.* **329,** 73–91
17. Raper, K. B. (1950) Stalk formation in *Dictyostelium*. *Science* **112,** 450
18. Mitra, B. N., Yoshino, R., Morio, T., Yokoyama, M., Maeda, M., Urushihara, H., and Tanaka, Y. (2000) Loss of a member of the aquaporin gene family, aqpA affects spore dormancy in *Dictyostelium*. *Gene* **251,** 131–139
19. Flick, K. M., Shaulsky, G., and Loomis, W. F. (1997) The wacA gene of *Dictyostelium discoideum* is a developmentally regulated member of the MIP family. *Gene* **195,** 127–130
20. Watts, D. J., and Ashworth, J. M. (1970) Growth of myxameobae of the cellular slime mould *Dictyostelium discoideum* in axenic culture. *Biochem. J.* **119,** 171–174
21. Hansen, M., Kun, J. F., Schultz, J. E., and Beitz, E. (2002) A single, bifunctional aquaglyceroporin in blood-stage *Plasmodium falciparum* malaria parasites. *J. Biol. Chem.* **277,** 4874–4882
22. Klammt, C., Löhr, F., Schäfer, B., Haase, W., Dötsch, V., Rüterjans, H., Glaubitz, C., and Bernhard, F. (2004) High level cell-free expression and specific labeling of integral membrane proteins. *Eur. J. Biochem.* **271,** 568–580
23. Klammt, C., Schwarz, D., Fendler, K., Haase, W., Dötsch, V., and Bernhard, F. (2005) Evaluation of detergents for the soluble expression of $\alpha$-helical and $\beta$-barrel-type integral membrane proteins by a preparative scale individual cell-free expression system. *FEBS J.* **272,** 6024–6038
24. Schneider, B., Junge, F., Shirokov, V. A., Durst, F., Schwarz, D., Dötsch, V., and Bernhard, F. (2010) Membrane protein expression in cell-free sys-

tems. *Methods Mol. Biol.* **601,** 165–186
25. Zeidel, M. L., Nielsen, S., Smith, B. L., Ambudkar, S. V., Maunsbach, A. B., and Agre, P. (1994) Ultrastructure, pharmacologic inhibition, and transport selectivity of aquaporin channel-forming integral protein in proteoliposomes. *Biochemistry* **33,** 1606–1615
26. Kai, L., Kaldenhoff, R., Lian, J., Zhu, X., Dötsch, V., Bernhard, F., Cen, P., and Xu, Z. (2010) Preparative scale production of functional mouse aquaporin 4 using different cell-free expression modes. *PLoS ONE* **5,** e12972
27. Grimbleby, F. H., and Ntailianas, H. A. (1961) Binding of trichloroacetic acid by protein. *Nature* **189,** 835–836
28. Eichinger, L., Pachebat, J. A., Glöckner, G., Rajandream, M. A., Sucgang, R., Berriman, M., Song, J., Olsen, R., Szafranski, K., Xu, Q., Tunggal, B., Kummerfeld, S., Madera, M., Konfortov, B. A., Rivero, F., Bankier, A. T., Lehmann, R., Hamlin, N., Davies, R., Gaudet, P., Fey, P., Pilcher, K., Chen, G., Saunders, D., Sodergren, E., Davis, P., Kerhornou, A., Nie, X., Hall, N., Anjard, C., Hemphill, L., Bason, N., Farbrother, P., Desany, B., Just, E., Morio, T., Rost, R., Churcher, C., Cooper, J., Haydock, S., van Driessche, N., Cronin, A., Goodhead, I., Muzny, D., Mourier, T., Pain, A., Lu, M., Harper, D., Lindsay, R., Hauser, H., James, K., Quiles, M., Madan Babu, M., Saito, T., Buchrieser, C., Wardroper, A., Felder, M., Thangavelu, M., Johnson, D., Knights, A., Loulseged, H., Mungall, K., Oliver, K., Price, C., Quail, M. A., Urushihara, H., Hernandez, J., Rabbinowitsch, E., Steffen, D., Sanders, M., Ma, J., Kohara, Y., Sharp, S., Simmonds, M., Spiegler, S., Tivey, A., Sugano, S., White, B., Walker, D., Woodward, J., Winckler, T., Tanaka, Y., Shaulsky, G., Schleicher, M., Weinstock, G., Rosenthal, A., Cox, E. C., Chisholm, R. L., Gibbs, R., Loomis, W. F., Platzer, M., Kay, R. R., Williams, J., Dear, P. H., Noegel, A. A., Barrell, B., and Kuspa, A. (2005) The genome of the social amoeba *Dictyostelium discoideum*. *Nature* **435,** 43–57
29. Liu, L. H., Ludewig, U., Gassert, B., Frommer, W. B., and von Wirén, N. (2003) Urea transport by nitrogen-regulated tonoplast intrinsic proteins in *Arabidopsis*. *Plant Physiol.* **133,** 1220–1228
30. Sui, H., Han, B. G., Lee, J. K., Walian, P., and Jap, B. K. (2001) Structural basis of water-specific transport through the AQP1 water channel. *Nature* **414,** 872–878
31. Törnroth-Horsefield, S., Wang, Y., Hedfalk, K., Johanson, U., Karlsson, M., Tajkhorshid, E., Neutze, R., and Kjellbom, P. (2006) Structural mechanism of plant aquaporin gating. *Nature* **439,** 688–694
32. Gupta, R., Jung, E., Gooley, A. A., Williams, K. L., Brunak, S., and Hansen, J. (1999) Scanning the available *Dictyostelium discoideum* proteome for O-linked GlcNAc glycosylation sites using neural networks. *Glycobiology* **9,** 1009–1022
33. Yasui, M., Hazama, A., Kwon, T. H., Nielsen, S., Guggino, W. B., and Agre, P. (1999) Rapid gating and anion permeability of an intracellular aquaporin. *Nature* **402,** 184–187
34. Beitz, E., Pavlovic-Djuranovic, S., Yasui, M., Agre, P., and Schultz, J. E. (2004) Molecular dissection of water and glycerol permeability of the aquaglyceroporin from *Plasmodium falciparum* by mutational analysis. *Proc. Natl. Acad. Sci. U.S.A.* **101,** 1153–1158
35. Haynes, P. A. (1998) Phosphoglycosylation. A new structural class of glycosylation? *Glycobiology* **8,** 1–5
36. Uzcategui, N. L., Szallies, A., Pavlovic-Djuranovic, S., Palmada, M., Figarella, K., Boehmer, C., Lang, F., Beitz, E., and Duszenko, M. (2004) Cloning, heterologous expression, and characterization of three aquaglyceroporins from *Trypanosoma brucei*. *J. Biol. Chem.* **279,** 42669–42676
37. Beitz, E. (2005) Aquaporins from pathogenic protozoan parasites. Structure, function and potential for chemotherapy. *Biol. Cell* **97,** 373–383
38. Bapteste, E., Brinkmann, H., Lee, J. A., Moore, D. V., Sensen, C. W., Gordon, P., Duruflé, L., Gaasterland, T., Lopez, P., Müller, M., and Philippe, H. (2002) The analysis of 100 genes supports the grouping of three highly divergent amoebae: *Dictyostelium*, *Entamoeba*, and *Mastigamoeba*. *Proc. Natl. Acad. Sci. U.S.A.* **99,** 1414–1419
39. Tamás, M. J., Karlgren, S., Bill, R. M., Hedfalk, K., Allegri, L., Ferreira, M., Thevelein, J. M., Rydström, J., Mullins, J. G., and Hohmann, S. (2003) A short regulatory domain restricts glycerol transport through yeast Fps1p. *J. Biol. Chem.* **278,** 6337–6345
40. Fischer, G., Kosinska-Eriksson, U., Aponte-Santamaría, C., Palmgren, M., Geijer, C., Hedfalk, K., Hohmann, S., de Groot, B. L., Neutze, R., and Lindkvist-Petersson, K. (2009) Crystal structure of a yeast aquaporin at 1.15 ångstrom reveals a novel gating mechanism. *PLoS Biol.* **7,** e1000130
41. Marchesini, N., Ruiz, F. A., Vieira, M., and Docampo, R. (2002) Acidocalcisomes are functionally linked to the contractile vacuole of *Dictyostelium discoideum*. *J. Biol. Chem.* **277,** 8146–8153
42. Nishihara, E., Yokota, E., Tazaki, A., Orii, H., Katsuhara, M., Kataoka, K., Igarashi, H., Moriyama, Y., Shimmen, T., and Sonobe, S. (2008) Presence of aquaporin and V-ATPase on the contractile vacuole of *Amoeba proteus*. *Biol. Cell* **100,** 179–188
43. Montalvetti, A., Rohloff, P., and Docampo, R. (2004) A functional aquaporin co-localizes with the vacuolar proton pyrophosphatase to acidocalcisomes and the contractile vacuole complex of *Trypanosoma cruzi*. *J. Biol. Chem.* **279,** 38673–38682
44. Zhang, Z., Chen, Z., Song, Y., Zhang, P., Hu, J., and Bai, C. (2010) Expression of aquaporin 5 increases proliferation and metastasis potential of lung cancer. *J. Pathol.* **221,** 210–220
45. Habermann, B. (2004) The BAR-domain family of proteins: a case of bending and binding? *EMBO Rep.* **5,** 250–255
46. Beitz, E. (2000) T(E)Xtopo. Shaded membrane protein topology plots in LAT(E)X2epsilon. *Bioinformatics* **16,** 1050–1051